Journal of the Mechanical Behavior of Biomedical Materials 99 (2019) 47–55

Contents lists available at ScienceDirect

Journal of the Mechanical Behavior of Biomedical Materials

journal homepage: www.elsevier.com/locate/jmbbm

Production and characterisation of novel phosphate glass fibre yarns, textiles, and textile composites for biomedical applications

Yunqi Wang[a], Xiaoling Liu[b,c], Chenkai Zhu[b,c], Andrew Parsons[e], Jinsong Liu[f], Songlin Huang[f], Ifty Ahmed[g], Chris Rudd[b,c], Nusrat Sharmin[b,c,d,*]

[a] International Doctoral Innovation Centre, University of Nottingham Ningbo China, Ningbo, 315100, China
[b] Ningbo Nottingham International Academy for the Marine Economy and Technology, University of Nottingham Ningbo China, Ningbo, 315100, China
[c] Ningbo Nottingham New Materials Institute, University of Nottingham Ningbo China, Ningbo, 315100, China
[d] Department of Chemical and Environmental Engineering, University of Nottingham Ningbo China, Ningbo, China
[e] Composites Research Group, Healthcare Technologies, Faculty of Engineering, University of Nottingham, NG7 2RD, UK
[f] Department of Technology, Sinoma Co., Ltd., 198 Tongtian Road, Nanjing, 211100, China
[g] Advanced Materials Research Group, Healthcare Technologies, Faculty of Engineering, University of Nottingham, Nottingham, NG7 2RD, UK

ARTICLE INFO

Keywords:
Phosphate glass
Fibre
Yarn
Textile
Biocomposite
Mechanical properties

ABSTRACT

This work presents manufacturing, processing and characterisation of the phosphate glass fibre (PGF) products for biomedical applications, including multifilament PGF strands, yarns and textiles, and PGF textile composites. The multifilament production of PGF strands was achieved using a 50-nozzle bushing. PGF yarns, with a linear density of 87 tex, a twist angle of 14° and a tensile strength of 0.29 N/tex, were produced by combining 8 fibre strands using the ring-spinning method. PGF textiles, with a width of 15 mm and a thickness of 0.36 mm, were prepared using an inkle loom. The maximum flexural strength and modulus of unidirectional (UD) composites with a fibre volume fraction of ~17% were 262 ± 11 MPa and 10.4 ± 0.2 GPa, respectively. PGF textile composites with a fibre volume fraction of ~21% exhibited mechanical properties of 176 ± 13 MPa for flexural strength and 8.6 ± 0.6 GPa for flexural modulus. Despite the UD and textile composites having almost an equivalent amount of fibres in the 0 direction, the crimp of the yarns was found to contribute to the significantly lower flexural properties of the textile composites in comparison with the unidirectional (UD) composites. Additionally, the processing conditions such as processing temperature and time were found to have a strong effect on the mechanical properties of the resultant composite products. The number-average molecular weight of PLA was also found to reduce by 13% and 19% after the production of PLA films and PLA plates, respectively, in comparison with the as-received PLA pellets.

1. Introduction

Conventional rigid medical implant devices can cause inflammatory responses in the body due to the corrosion and release of metal ions (Patel and Gohil, 2012). Furthermore, the extreme higher modulus (up to seven times) of the implants in comparison with the underlying hard tissues can lead to stress shielding effects (Bauer and Schils, 1999; Ramakrishna et al., 2001; Thompson and Hench, 1998), where the metal implants carry most of the load, leading to osteoporosis of bone and a slow healing process (~1–2years) (Ramakrishna et al., 2001; Ferguson et al., 1996). The interest in phosphate glass fibre (PGF) reinforced biodegradable composites for implant materials keeps increasing due to their unique chemical and mechanical properties. In comparison with conventional rigid implants, the PGF composites can provide several significant advantages: the mechanical properties of PGF composites are close to those of human cortical bone (Ahmed et al., 2004a, 2004b; Knowles et al., 2001); they can degrade gradually over the bone healing period to allow for load transfer to the underlying bone (therefore, stress shielding and osteopenia can be virtually eliminated (Scholz et al., 2011; Middleton and Tipton, 2000; Athanasiou et al., 1998)); they can be dissolved completely in aqueous media (eliminating the need for removal surgery); and the breakdown products would not elicit inflammatory response of body (Ahmed et al., 2004a, 2004b; Scholz et al., 2011; Middleton and Tipton, 2000). Moreover, PGFs have the potential to be used for stem cells transportation and help to regenerate damaged and diseased muscle (Ahmed et al., 2004b, 2004c). Additionally, PGF composites are potentially applicable as drug carriers for hard-tissue regeneration and wound-

* Corresponding author. Room 339, Sir Peter Mansfield Building, University of Nottingham Ningbo China, 199 Taikang East Road, Ningbo, 315100, China.
E-mail address: nusrat.sharmin@nottingham.edu.cn (N. Sharmin).

https://doi.org/10.1016/j.jmbbm.2019.07.017
Received 18 December 2018; Received in revised form 5 June 2019; Accepted 18 July 2019
Available online 19 July 2019

healing (Kim et al., 2005). Based on these advantages, biodegradable PGFs composite materials have huge potential to be used for bone fracture-fixation devices.

Several studies (Ahmed et al., 2009, 2011; Felfel et al., 2012; Han et al., 2013; Parsons et al., 2009) have investigated the manufacture of PGF composites using fibrous preforms such as random chopped mat, 0–90° and unidirectional (UD) mats to produce composites via a compression moulding method. All these preforms were made from single filament fibres using an experimental single-tip bushing, which can be quite a time consuming process. Empirically, a high level of processing skill is required to make these kinds of composites due to the loose structure of preforms which can result in difficulties in storage, transportation, and arranging fibres evenly in the mould during processing.

As such, both the scale-up production of PGF and preforms with compact and defined architecture would be required, especially for achieving commercialisation. Recently, an industrially relevant scale production of multifilament fibres was achieved with a pilot plant in co-operation with Sinoma Ltd. (Nanjing, China), using the phosphate-based glass (PBG) formulation (glass code P48B12) developed by Zhu et al. (2017). The additional advantage of multifilament fibre drawing is the manufacture of compact preforms, such as textiles. In a textile mat the fibres could be held together in the form or size required without the involvement of a polymer matrix, hence, they can be easily handled, transported and processed in comparison to non-woven preforms (Adumitroaie and Barbero, 2011; Cox and Flanagan, 1997a; Jean et al., 2008; K Naik and S Shembekar, 1992). Textiles can also be easily manufactured into desired complicated geometrical shapes using a large number of fabric architectures (Adumitroaie and Barbero, 2011; Kravaev et al., 2013). Additionally, textile composites are more damage tolerant than UD composites due to the interlacing tows which can provide resistance to crack propagation (Jean et al., 2008; K Naik and S Shembekar, 1992; Goyal and Whitcomb, 2008; Abot et al., 2011; Guagliano and Riva, 2001; Naik et al., 2000; Zheng et al., 1999).

Twisting of yarns is an engineering requirement for textile yarn production in order to avoid the separation of strands into individual filaments or bundles during textile processing due to the lack of lateral cohesion among dry fibre strands, and to improve the abrasion resistance of yarns (Naik and Madhavan, 2000; Naik and Singh, 2001; Jebastin Rajwin et al., 2012; Naik and Kuchibhotla, 2002; Zhang and Miao, 2010). However, the twist tightens the structure of yarns and consequently can lead to difficulty of resin impregnation (Zhang and Miao, 2010). Moreover, the PGF textile/PLA composites were produced via compression moulding techniques in the current study, hence, the thermal degradation behaviour of PLA would also need to be considered while it is being processed (Carrasco et al., 2011; Lim et al., 2008). Ideally, the temperature and processing time should be adjusted in order to ensure the melted polymer can sufficiently penetrate through the PGF textile reinforcements, wetting it out completely before rapid cooling down to room temperature to avoid surplus thermal degradation during compression moulding.

The aim of this work was to achieve multifilament PGF production and to manufacture both PGF textiles and textile composites for biomedical applications. Two processing conditions with different heating temperatures and processing times were used during compression moulding. Hence, the effects of the processing conditions on the mechanical properties of PGF textile reinforced PLA composites have also been investigated. This work represents the first data reported on processing, manufacturing and characterisation of PGF strands and yarns.

2. Materials and methods

2.1. Industrial scale production of phosphate glass

The composition of glass code P48B12Na1 (Zhu et al., 2017) was used in the present study (see Table 1). Ten kilograms of glass was produced at Sinoma Co., Ltd (China) using phosphorous pent-oxide (P_2O_5) (Shanghai Lingfeng Chemical Reagent Co., Ltd., China), calcium hydrogen phosphate di-hydrate ($CaHPO_4{\cdot}2H_2O$)(Shanghai Shisihewei Chemical Co., Ltd., China), di-hydrogen sodium phosphate di-hydrate ($NaH_2PO_4{\cdot}2H_2O$) (Tianjin Kemiou Chemical Reagent Co., Ltd., China), magnesium hydrogen phosphate tri-hydrate ($MgHPO_4.3H_2O$) (Shanghai Shenbo Chemical Co., Ltd., China), boric acid (H_3BO_3) (Shanghai Jingxu Industrial Co., Ltd., China), and iron phosphate tetra-hydrate ($FePO_4{\cdot}4H_2O$) (Shenzhen Shek Tin Technology Co., Ltd., China) in powder form. Appropriate amount of precursors were weighed out and pre-mixed in a stainless steel receptacle, then transferred into a corundum brick furnace and heated from room temperature to 1100 °C for ~10 h to remove the residual H_2O. Then the temperature was held at 1100 °C for another ~6 h to ensure that the mixture was fully melted. The molten glass was then left overnight to cool down to room temperature and was removed from the furnace by chiselling the glass into small pieces.

Table 1
Composition of P48B12Na1 used for glass and fibre production (Zhu et al., 2017).

Composition	P_2O_5	B_2O_3	MgO	CaO	Na_2O	Fe_2O_3
Content (mol %)	48	12	20	14	1	5

2.2. Production of multifilament glass fibres

Multifilament PBG fibres were produced at Sinoma Co., Ltd (China) utilizing an in-house constructed 50-tips platinum bushing, which was electrically-heated. The fibre forming temperature (T_f) and liquidus temperature (T_l) of P48B12Na1 glass were reported to be 903 °C and 1015 °C respectively (Zhu, 2016). Initially, the glass was pre-heated in a corundum brick furnace to 1050 °C for ~3 h using SiC heaters (SCR, Zhenzhou Songshan Heating Elements Co., Ltd, China) and then further heated to ~1060 °C and held at this temperature for ~30 min to achieve equilibrium. The temperature of the bushing at the bottom of the furnace during fibre drawing was adjusted to be within a range of 1050–1075 °C throughout the fibre production process. Continuous PGFs were obtained by rapid mechanical attenuation (i.e. rapidly drawn) and quenching of PBG molten drops exuding from the tips of the bushing. A water-soluble epoxy resin (confidential product developed by Sinoma) was employed as sizing, which provided surface protection of fibres and facilitated ease of textile fabrication. The biocompatibility of this sizing is still under investigation. Finally, the fibre strands (50 filaments) were wound onto a removable tube on a collet which was spun at a speed of 3000 rpm for 10 min to achieve a sufficient thickness of the fibre product (referred to as a “cake” (Lowenstein, 1973)). The wet cakes were dried at room temperature for ~12 h before further processing.

2.3. Production of yarns

Eight PGF multifilament strands (from the cakes produced) were combined using a conventional ring spinning method for yarn production (Gowda et al., 2010). Two threads were produced first by twisting and twinning fibre strands using a twisting machine (CGKV550A, Yichang Jingwei Textile Machinery Co., Ltd., China) with a twist of 55 T/m in “S” direction. The twisted threads were then plied and wound onto a milk-bottle shaped bobbin using another twisting machine (150B–I, Luoyang Building Materials Mechanical Co., Ltd.) with a same twist of 55 T/m in “Z” direction (the opposite direction of “S” direction) in order to balance the torque and avoid any stress in the yarn.

2.4. Characterisation of fibre strands and yarns

2.4.1. Determination of the linear density of fibres strands and yarns

The linear density of the PGF basic strands, and the subsequently produced yarns were determined according to the standard ISO 1889: 2009 (Reinforcement yarns-Deter, 2009a). 200-meter fibre strand/yarn specimens were collected using a measuring reel (YG086, Changzhou No.2 Textile Machinery Co., Ltd., China) and weighed. The measurement was accomplished in triplicate using three different specimens, which were based on a sampling of ~10% of the entire strands. The linear density of the yarn was calculated using Eq. (1):

$$L = \frac{1000m}{l} \quad (1)$$

where, L is the linear density of yarn, m is the weight of the sample in g, and l is the length of the sample in metres. In the present study, l was 200 m.

2.4.2. Density measurement

Density of both PBGs and PGFs was determined using a helium pycnometer (Gas Pyrometer Accupyc 1330, Micrometrics, USA). The density was measured at room temperature with a relative humidity of ~50%. The pycnometer was calibrated using a standard calibration ball with a volume of 3.18551 cm^3 (errors within a range of ± 0.05%). Triplicate density measurements were conducted using different PBG or PGF samples.

2.4.3. Determination of twist of yarns

The twist of PGF yarns was measured in accordance with the standard ISO 1890:2009 (Reinforcement yarns-Deter, 2009b) using a twist tester (Y331A1, Changzhou Second weaving instrument Co., Ltd., China). Yarn specimens with a length of 0.5 m were loaded for measurement with a standard tension of 0.25 cN/tex. The test was repeated three times.

2.4.4. Determination of breaking force and breaking elongation of fibre strands and yarns

Fibre strands and yarns were acclimatised at an ambient temperature of 23 ± 2 °C with a relative humidity of 50 ± 10% for 6 h before testing. Ten specimens of fibre strands and yarns were tested in accordance with the standard ISO 3341: 2000 (Textile glass-Yarns-Deter, 2000) using a tensile test machine (CSS-44020, Changchun Research Institute for Mechanical Science Co., Ltd., China) with a gauge length of 250 mm. The test specimen was firstly secured by the clamps, straightened and aligned parallel to the direction of applied force, and then tested with an extension rate of 200 mm/min. The breaking force (in N) of the fibre strands was divided by their linear density (in tex) to obtain the strength in N/tex.

2.5. Characterisation of textiles

PGF plain weave textiles with a width of 1.5 cm were produced manually using an inkle loom following the procedures described by Bress (Helene BressInkle, 1975). The numbers of yarns per unit length in both the warp and the weft directions were counted using a traversing microscope (Y511B, Changzhou Textile Instrument Co., Ltd, China) in accordance with test method B of the standard ISO 4602:2010 (Reinforcements–Woven fab, 2010), and was calculated using the following Eq. (2):

$$N_i = \frac{n_1}{a_i} \quad (2)$$

where, N_i (i is either warp or weft) stands for the number of yarns per centimetre, n_1 is the number of yarns counted and a_i is the measured length of the textile, in cm.

The distance over which the yarns were to be counted was fixed at 5 cm for the warp direction, and 1 cm for the weft direction due to the limited width (~1.5 cm) of the textile. Measurements were accomplished at four different positions along the warp and weft directions.

2.6. Production of PLA and composite plates

2.6.1. Production of unidirectional mats

Uni-directional (UD) fibre mats were produced using PGF yarns. The yarns were manually rolled onto a drum with a diameter of 30 cm and spray coated (to maintain alignment) using an aerosol spray bottle with 50 ml of PLA solution (3251D, NatureWorks LLC., U.S.; 0.05 g/ml; dissolved in chloroform). The drum was then left in a fume hood for 2 h to allow the chloroform to evaporate. The dried UD sheet was then removed from the drum and cut into square shaped sheets (140 × 15 mm^2) for composite manufacturing.

2.6.2. Production of PLA films and composite plates

The 3251D PLA pellets provided by NatureWorks LLC was used in the present study for the production of composites due to their low relative viscosity, which is 2.5 (Ingeo™ Biopolymer 3251, 2011), is lower than the other series (within the range of 2.5–4). Therefore, the PLA 3251D was considered to be beneficial for impregnation (i.e. fibre wet out) during compression moulding.

PLA films with a thickness of approximately 0.2 mm were prepared by compression moulding PLA pellets, which were dried at 50 °C in a vacuum oven for 24 h before use. For each film, 5 g of PLA pellets were covered with polytetrafluoroethylene (PTFE) release films and placed between two 6 mm thick aluminium plates. The plates were then placed into a hydraulic press (J. R. Dare Ltd, U.K.) at 190 °C and preheated for 10 min followed by pressing at 10 bar for 30 s. After that the plates were transferred onto a cooling press (Daniels Upstroke Press, U.K.) and pressed at the same pressure to cool down to room temperature. These films were cut into square sheets with dimensions of 140 × 15 mm^2 and dried at 50 °C in a vacuum oven for 24 h before composite production.

To produce PLA plates, the prepared films were then placed into a frame mould with a cavity size of 140 × 15 × 2 mm^3 and covered with PTFE release films. Two different PLA plates (coded as PLA-PC1 and PLA-PC2) were produced with two different processing conditions (referred to as PC 1 and PC 2), as listed in Table 2. These processing conditions were chosen based on the processing conditions used in the other literatures (Ahmed et al., 2011; Ali Ashter, 2016) for compression moulding of PLA composites. After the heat compression, the plates were transferred onto a cooling press (Daniels Upstroke Press, U.K.) to cool down to the room temperature under a load of 40 bar.

The composites in the current study were reinforced using ~20 vol % of UD mats or textiles. The UD and textile preforms were kept in a vacuum oven at 50 °C for 24 h before further processing. To produce composites using a film/laminate-stacking method, reinforcement fibre (either UD or textile) layers were alternatively sandwiched between PLA films and placed into a 2 mm thick frame mould covered with PTFE

Table 2
The processing conditions (PC 1 and PC 2) used for PLA and textile composite samples preparation.

Processing condition (PC) code	Temperature (°C)	Preheat time (min)	Compression time (min)	Compression pressure (bar)
PC 1	200	15	15	40
PC 2	180	10	10	40

films. Two groups of textile composites (referred to as TC-PC1 and TC-PC2) and two groups of UD composites (referred to as UD-PC1 and UD-PC2) were produced in a similar procedure to the PLA plates.

2.7. Characterisation of composite plates

2.7.1. Flexural tests

The flexural properties (flexural strength and modulus) of composite specimens (40 × 15 × 2 mm^3) were determined in accordance with the standard ISO 14125: 1998 (Fibre-reinforced plastic, 1998) via three-point bending tests using an Instron 5969. A cross-head speed of 1 mm/min and a load cell of 1 kN were used. The distance between the supporting rollers was 32 mm. The load was applied perpendicular to the UD fibres/warp yarns in the composites. The flexural tests were carried out in triplicate (n = 3).

2.7.2. Burn off tests

The actual fibre volume fractions of composites investigated were determined via burn off tests in accordance with the standard ASTM D2584-11 (Standard test mechod for, 2584). Composite samples (n = 3) were placed into a muffle furnace (SX2-10-12, Shanghai Suopu Instrument Co., Ltd., China) at a temperature of 550 °C for 3 h, ensuring complete combustion of resin.

2.7.3. Gel permeation chromatography (GPC) study

Thermal degradation of PLA during compression moulding was studied by monitoring the changes of molecular weight in the neat PLA plates using GPC tests in accordance with the standard DIN 55672-1-2007 (Gel permeation chromatogr, 2007). GPC tests were conducted by Shanghai Boyan Testing Technical Service Co., Ltd., China. GPC was performed using a refractive index detector (Waters 2414). Tetrahydrofuran was used as eluent. Tests was performed at 40 °C with a flow rate of 1 ml/min through Agilent PLgel 5 μm MIXED-C columns with a calibration range of 580–483,400 Da calibrated with poly (styrene) standards. GPC data was analysed using the Breeze software. Note that the molecular weight of PLA matrix in the fibres reinforced composites was assumed to be close to that of the correlated neat PLA plates produced using the same processing conditions.

2.8. Scanning electron microscope (SEM) study

The PGF textiles and composites were observed using a scanning electron microscope (Vega 3, Tescan, China) operated in secondary electron mode. The cross sections of fractured composites after flexural tests were polished before being coated with platinum using a sputter coater (SC7620, Quorum, UK).

3. Results

3.1. Production of PGF fibres strands and yarns

Approximately 3 kg of PGF strands were obtained from 8 kg of PBG bulk glass, which were subsequently converted into of PGF yarns (see Fig. 1). The details of both single strand and yarn are listed in Table 3. The average linear density of a single strand determined using a measuring reel was 12.5 tex. The actual linear density of the yarn, which combined 8 PGF strands, was 86.3 tex, which was ~14 tex lower than the theoretical linear density (100 tex). The tensile strength of resultant yarn was 0.29 N/tex, which was slightly lower ($P > 0.05$) than that of single strand (0.31 N/tex). The twist angle of yarns was estimated to be ~14° by following the methods of both Naik et al. (Naik and Madhavan, 2000) and Cox et al. (Cox and Flanagan, 1997b).

3.2. Characterisation of PGF textiles

A manually woven PGF textile was produced with a width of 15 mm and a length of ~530 mm (see Fig. 2). The warp system crack due to the yarn damages was rarely observed during inkle weaving. The yarn counts were 22.8 ± 0.1/cm and 6.2 ± 0.1/cm for warp and weft threads, respectively.

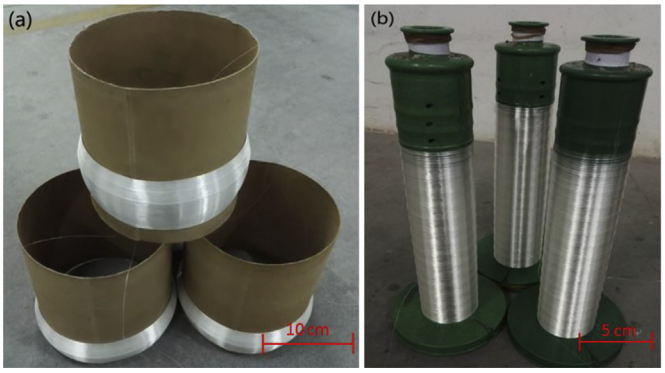

Fig. 1. (a) cakes with fibre strands; (b) yarns would on milk-bottle bobbins.

Table 3
Details of single PGF strand and yarn.

Thread type	Strand	Yarn
Strands	1	8
Linear density (tex)	12.5 ± 0.6	87.3 ± 2.7
Tensile strength (N/tex)	0.31 ± 0.03	0.29 ± 0.02
Actual twist (T/m)	N/A	52 ± 2
Twist angle (°)	N/A	14.1 ± 0.1

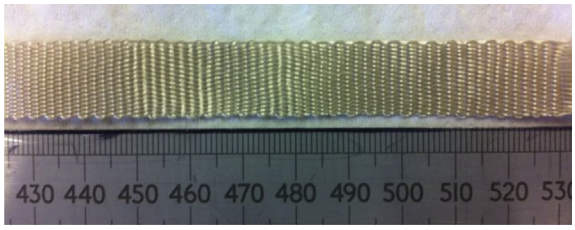

Fig. 2. PGF textiles produced with a length of ~530 mm.

3.3. Burn off tests

The target and actual fibre volume fractions of UD and textile composites, and the calculated fibre volume fractions along the warp and weft directions of textile composites are listed in Table 4. For both UD and textile composites, no statistically significant difference ($P > 0.05$) in fibre volume fraction was seen with changing processing conditions. Meanwhile, the burn off test confirmed that the real fibre volume fractions for all of the composites were within an acceptable range (± 3%). The fibre volume fractions for all composites in the longitude direction (i.e. either UD or warp direction) were found to be within a similar range (17.3 ± 0.3 vol %).

Table 4
The target ($V_{f,t}$) and actual (V_f) fibre volume fractions of UD and textile composites produced using two different processing conditions.

Composite Code	$V_{f,t}$ (%)	V_f (%)	$V_{f,warp}$ (%)	$V_{f,weft}$ (%)
UD-PC1	20	17.6 ± 0.7	N/A	N/A
UD-PC2	20	17.2 ± 0.7	N/A	N/A
TC-PC1	20	21.7 ± 0.3	17.1	4.6
TC-PC2	20	21.4 ± 0.3	16.9	4.5

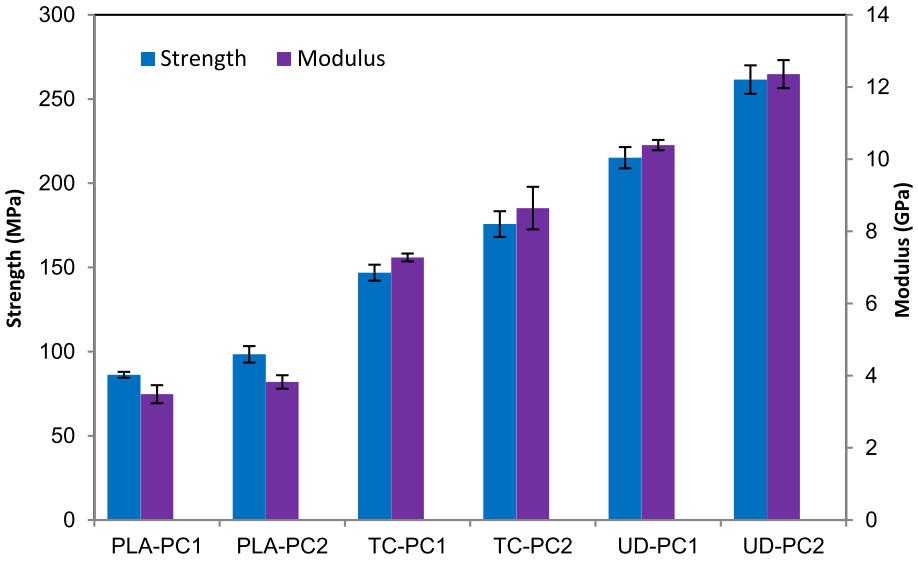

Fig. 3. Flexural strength and modulus of PLA, textile and UD composite plates, produced using two different processing conditions during compression moulding.

3.4. Flexural properties of composites

A comparison of flexural strength and modulus for PLA plate, UD composites and textile composites produced using two different processing conditions during compression moulding is shown in Fig. 3. The flexural strengths of PLA-PC1, TC-PC1 and UD-PC1 plates were 86 MPa, 147 MPa and 215 MPa, respectively, which increased to 98 MPa ($P > 0.05$), 176 MPa ($P < 0.05$), and 262 MPa ($P < 0.05$) for PLA-PC2,TC-PC2 and UD-PC2 plates, respectively. The flexural modulus of PLA-PC1, TC-PC1 and UD-PC1 plates were 3.5 GPa, 7.3 GPa and 10.4 GPa, respectively, which increased to 3.8 GPa ($P > 0.05$), 8.6 GPa ($P > 0.05$), and 12.4 GPa ($P > 0.05$) for PLA-PC2, TC-PC2 and UD-PC2 plates, respectively. The textile composites (TC-PC1 and TC-PC2) were seen to exhibit ~32% lower in both flexural strength and modulus in comparison with the corresponding UD composites (UD-PC1 and UD-PC2) produced using the same processing conditions. Delamination was observed for TC-PC1 during flexural tests as shown in Fig. 4. Brittle failure occurred with all the other types of plate.

3.5. SEM analysis

The morphology of the PGF textiles produced is shown in Fig. 5. A compact plain weave architecture was seen without gaps between adjacent yarns. Straight orientation of filaments was observed which confirmed that sufficient tension was applied during inkle weaving. Few broken fibres were observed.

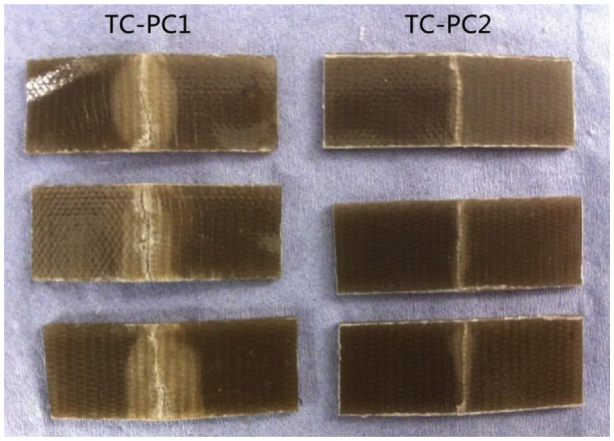

Fig. 4. Textile composites (TC-PC1 and TC-PC2) after flexural tests. Delamination was seen for TC-PC1.

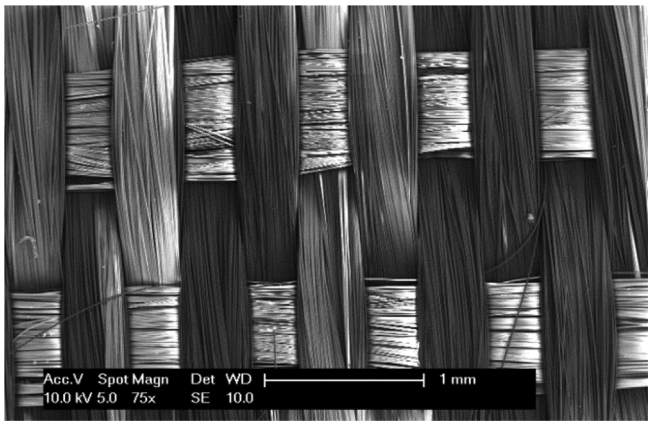

Fig. 5. SEM image of the PGF textile surface. No gaps were seen between adjacent yarns and few broken fibres were observed.

The polished cross-sections of the composites after flexural tests are shown in Fig. 6. It was seen that the fibres were well wet-out within the matrix for all the composite samples. Very few voids were found. The textile structure was evident in Fig. 6(c) and (d). Elliptical cross-sections of yarns in textile composites were observed. Polymer rich regions were also observed for both UD and textile composites.

3.6. GPC study

The thermal degradation of the polymer matrix during processing was investigated by monitoring the variation in molecular weight between PLA pellets and films and plates as shown in Fig. 7. The number-average molecular weight (M_n) was used for the characterisation which should correlate with the mechanical properties of solid polymers (KumarRakesh, 2003). The original M_n of PLA (pellets) was 104 kDa. After being processed in to films, ~10% reduction in M_n was seen. The processing of PLA films into PLA plates resulted in a further reduction of M_n to 57 kDa for the plate PLA-PC1, which was ~23% lower than PLA-PC2 plates (74 kDa).

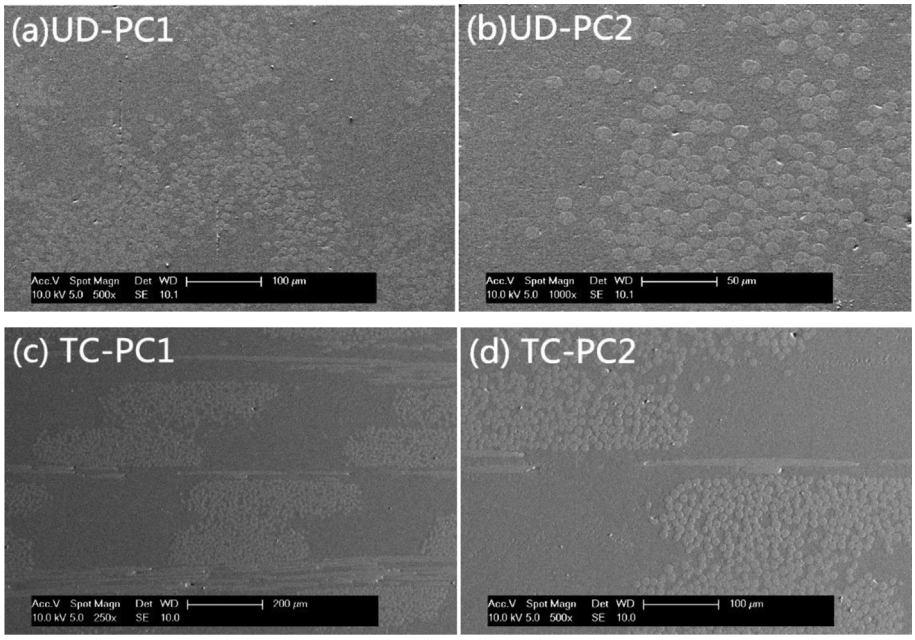

Fig. 6. The SEM micrographs of the cross sections of composites: (a) UD-PC1; (b) UD-PC2; (c) TC-PC1; (4) TC-PC2.

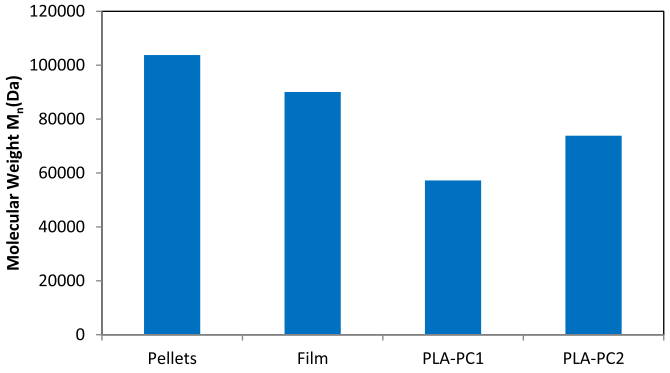

Fig. 7. Molecular weight of PLA pellets, films, and PLA plates produced under two different processing conditions (PLA-PC1 and PLA-PC2). Errors were within 0.3% (Gel permeation chromatogr, 2007).

4. Discussion

4.1. Manufacturing of PGF strands and yarns

The first data on processing, manufacturing and characterisation of PGF strands and yarns has been obtained in the present study. During the manufacturing process, the interruption of fibre drawing appeared to occur randomly at various bushing tip locations whenever fresh bulk glass was added to the furnace to maintain the height of molten glass in the similar level. This interruption in the fibre drawing could be due to the decrease in glass melt temperature when solid glass was added which potentially resulted in the increased viscosity of glass melts. The increased viscosity would decrease the flow rate of glass melt through the bushing (Loewenstein, 1975), and consequently contribute to the filament breakages at the bushing tips.

The PGF strands were not dried before ring-spinning the yarns as the dried PGF strand was too brittle and the entire strand system was prone to damage during the unloading of fibre strands from the cakes. Additionally, a few amount of fibre strands (~0.5 kg) were unusable mainly due to the strand system failure during unloading of the wet fibre strands from cakes and ring-spinning of yarns. The overall material utilization rate from bulk glass to the yarn products was ~30%.

4.2. Characterisation of PGF strands and yarns

The average linear density of a single fibre strand was 12.5 tex (see Table 3). However, it was found that the yarn, which combined 8 strands of filaments, had a linear density of only 87.3 tex as opposed to the expected 100 tex. This could be as a result of variation in the linear densities of the fibre strands caused by the fibre drawing interruptions occurring at bushing tips, as discussed above in Section 4.1. However, given the relatively low error in the measured tex of the individual strands (see Table 3), this is unlikely to be the only factor. Additional loss almost certainly occurred due to flyaway of broken fibres during the twisting process.

Yarns are normally twisted to increase the lateral cohesion of the filaments and also for ease of handling (Naik and Madhavan, 2000; Naik and Singh, 2001; Naik and Kuchibhotla, 2002). The potential for micro damage within the yarns can be localized by twisting the yarns, resulting in a possible increase in the tensile strength of the yarn as compared to fibre strands (Naik and Madhavan, 2000; Naik and Singh, 2001; Jebastin Rajwin et al., 2012; Naik and Kuchibhotla, 2002). However, twisting can only increase the tensile properties of yarns up to a maximum level, with further increases in the twist leading to reduction in the tensile properties (Naik and Kuchibhotla, 2002; Chudoba et al., 2007). This is mainly due to the increased twist angle potentially leading to an increase in pre-straining of the filaments, which can have a negative effect on the tensile properties of the yarns (Naik and Singh, 2001; Naik and Kuchibhotla, 2002). Rocher et al. (2014) stated that a low yarn twist with a twist angle up to 7° could improve the breaking strength of glass fibre/polypropylene yarns (400 tex) in comparison with untwisted strands. When the twist angle was higher than 15°, the yarn breaking strength became lower in comparison with the untwisted strands (Rocher et al., 2014). The effect of twist on the mechanical properties of yarns and composites also depends on the nature and linear density of yarns. Chudoba et al. (2007) investigated the effects of linear density (640, 1200 and 2400 tex), twist (0, 10, 20, 40 and 60 turns/m) and loading rate (1–40%/min) on the tensile behaviour of alkali resistant glass yarns. They found that a twist level of 20 turns/m improved the tensile strength for all yarns investigated. Additionally, the effect on the tensile behaviour of yarns of a level of twist higher than 20 turns/m could be either beneficial or negative, depending mainly on the linear density (Chudoba et al., 2007). In the present

study, the tensile strength of fibre strands (~87 tex) was slightly reduced ($P > 0.05$) after yarn twisting (55 turns/m, see Table 3). Therefore, it could be concluded that the twist of 55 turns/m, which provided a yarn twisting angle of ~14° (see Section 3.1), overtwisted the yarns and reduced the tensile strength.

Despite the requirement of twist for producing textile yarns, it was noteworthy that twisted yarn can provide a negative impact to the mechanical properties of the resultant composites (Zhang and Miao, 2010; Miao and Christa Soong, 1995). Naik et al. (Naik and Kuchibhotla, 2002) reported that the E-glass yarn with a twist angle up to 5° could facilitate ease of textile fabrication without significantly compromising the strength of the woven fabric composites. Hence, the twist level of PGF yarns could be optimised to ~20 turns/m in the future studies, to give a twist angle of ~5° for a yarn with a linear density of 87 tex.

4.3. PLA plates, PGF textiles and textile composites

In the present study, PLA plates were produced as the control group by stacking and melt processing PLA films. The flexural strength and modulus of the PLA plates were within the range of 85–100 MPa and 3.5–3.8 GPa, respectively. These flexural properties of the PLA plates were comparable to the values reported by Felfel et al. (2012) and Han et al. (2013) (93–100 MPa for flexural strength and 3.8–5 GPa for modulus). Zhu et al. (2018) investigated the mechanical properties of resorbable UD composites comprising PLA matrix with the same PGF yarns used in the current study. They reported that the composites with a fibre volume fraction of ~20% provided 286 MPa and 13.8 GPa for flexural strength and modulus, respectively (Zhu et al., 2018). These values were close to values obtained for the UD-PC2 composites investigated in the current study (see Section 3.4).

PGF plain textiles were produced manually using an inkle loom as a short-term tool for the lab-scale fabrication. Values for flexural strength and modulus were within a range of 147–176 MPa and 7.3–8.6 GPa, respectively, as seen in Fig. 3. These values were comparable to values reported by Zhu et al. (2018) for a ~20 vol% PGF textile composite, which has a flexural strength of ~176 MPa and a modulus of ~8.6 GPa. These composites would provide mechanical properties similar to those of human cortical bones, which have a flexural strength within a range of 135–193 MPa (Fu et al., 2011). The fibre volume fractions for these initial composites are relatively low (~20 vol%) and an increase to around 40 vol% would be expected to almost double the modulus (Han et al., 2013), whereby the modulus of human cortical bone (10–20 GPa (Fu et al., 2011)) could be easily achieved.

The yarn content of PGF textiles was ~79% along the longitudinal (warp) direction (see Section 3.2). Therefore, the fibre volume fractions for textile composites in the warp direction were about 17%, which were close ($P > 0.05$) to the UD composites in the longitude direction (see Table 4). However, the strength of the textile composites was found to be ~32% ($P < 0.001$) lower than the UD composites produced using the same processing conditions (see Fig. 3). This revealed that the mechanical properties of the textile composites were affected heavily by the architecture of the textiles. Despite the advantages provided by textile preforms, such as the ease of handling and processing, and also the higher resistance to crack propagation as compared to UD preforms (Adumitroaie and Barbero, 2011; Cox and Flanagan, 1997a; Jean et al., 2008; K Naik and S Shembekar, 1992; Kravaev et al., 2013; Goyal and Whitcomb, 2008; Abot et al., 2011; Guagliano and Riva, 2001; Naik et al., 2000; Zheng et al., 1999), these textile architectures provided negative effects on the mechanical properties of the composites (when compared to UD composites) which was mainly due to the degree of crimp. Various studies (Goyal and Whitcomb, 2008; Zheng et al., 1999; Cox and Flanagan, 1997b; Naik, 1995; Barbero et al., 2005; Long et al., 2005) of textile composites stated that the yarn crimp can induce local stress concentration at the interlacing areas, leading to an increase in the rate of fibre damage accumulation during loading and the consequent reduction of the mechanical properties of the resultant composite materials. A larger crimp angle can lead to a greater drop in the mechanical properties (Naik, 1994).

Additionally, there were more resin-rich regions in textile composites as compared to the UD composites as observed in Fig. 6. These resin-rich regions were known to have a negative effect on the mechanical properties (Wisnom et al., 2007). The formation of polymer rich areas was mainly due to the nature of a woven structure that formed spaces and constrained PLA melts at the interlacing areas of yarns during processing.

4.4. Processing conditions

Instead of PLA pellets, PLA films were used for the production of neat PLA plates in order to ensure that the PLA control group has similar thermal history to those of the composites. This was an important consideration since PLA suffers degradation during melting, as evidenced by the significant reduction in M_n after processing (see Fig. 7). The variation of mechanical properties correlated well with the molecular weight of the PLA plates, for which the PLA-PC1 has a M_n approximately 22% lower than PLA-PC2. This rapid loss of molecular weight was responsible for the reduction of the polymer properties (Taubner and Shishoo, 2001; Yu et al., 2010; Södergård and Näsman, 1994).

The flexural strengths for UD and textile composites produced using processing condition 1 (see Table 2) were 17.7% ($P < 0.05$) and 16.4% ($P < 0.05$) lower than the composites produced using processing condition 2, as shown in Fig. 3. This difference is too large to be accounted for purely by the difference in matrix modulus or strength. Polished cross sections of the composites (see Fig. 6), indicated a good consolidation between PGF fibres and the PLA matrix (Lauke et al., 1998; Tanoglu et al., 2001). However, the delamination observed for TC-PC1 during flexural testing (see Fig. 4) would suggest a weaker fibre interface resulting from the higher temperature processing conditions. A number of studies (M Zhao and Takeda, 2000; Lauke et al., 1998; Tanoglu et al., 2001; Faulstich De Paiva et al., 2005; Mahmood, 2011; Van Rijswijk et al., 2009)have suggested that the delamination prior to matrix cracking indicates a weak fibre/matrix interface that cannot withstand the inter-laminar shear stresses necessary to realise the ultimate strength of the fibres. In this study, the molecular weights of the composite matrix polymers were assumed to be similar to those of the correlating PLA plates produced using the same processing conditions. Therefore, the lower inter-laminar shear properties of the PC1 composites could be due to their lower matrix molecular weight as compared to the PC2 composites.

Thus, it is suggested that the processing conditions (i.e. temperature, heating and compression time) should be optimized not only to ensure full wet-out of the fibres but also to minimize thermal degradation of the PLA matrix, since this appears to have a disproportionately large effect on the composite properties.

5. Conclusions

In this study, the industrial-scale multifilament production of PGF strands, yarns and textiles was achieved. The strands, yarns and textiles were characterized and composites were manufactured successfully in the lab. The low production yield of fibres (~3 kg from 8 kg bulk glass) indicated that it is necessary to further develop fibre drawing process. The twist level of PGF yarns should be optimised with literature suggesting that ~20 turns/m (which gives a twist angle of ~5°) should facilitate ease of PGF textile fabrication without over-twisting the yarn.

The crimp of the textiles was found to have a significant negative effect on the flexural properties of textile composites, as would be expected. It was also found that the processing conditions have a strong effect on the mechanical properties of the resultant composites. The temperature and processing time should be minimised to a level

sufficient for full wet-out of the fibres and consolidation without any surplus thermal degradation of matrix.

The PGF textiles were obtained by manual Inkle weaving in the present study. Industrial-scale weaving machines could be used to provide better control of tension during manufacture and should reduce the degree of pre-strain. Additionally, the biocompatibility of the sizing used in the present study should be investigated in the future.

Acknowledgement

The authors acknowledge the financial support from the International Doctoral Innovation Centre, Ningbo Education Bureau, Ningbo Science and Technology Bureau, and the University of Nottingham. This work was also supported by the UK Engineering and Physical Sciences Research Council [grant numbers EP/G037345/1 and EP/L016362/1]. The authors would also like to acknowledge the technical support from Sinoma Ltd., Nanjing, China.

Appendix A. Supplementary data

Supplementary data to this article can be found online at https://doi.org/10.1016/j.jmbbm.2019.07.017.

References

Abot, J.L., Gabbai, R.D., Harsley, K., 2011. Effect of woven fabric architecture on interlaminar mechanical response of composite materials: an experimental study. J. Reinf. Plast. Compos. 30 (24), 2003–2014.
Adumitroaie, Adi, Barbero, Ever J., 2011. Beyond plain weave fabrics – II. Mechanical properties. Compos. Struct. 93 (5), 1449–1462.
Ahmed, I., Collins, C.A., Lewis, M.P., Olsen, I., Knowles, J.C., 2004a. Processing, characterisation and biocompatibility of iron-phosphate glass fibres for tissue engineering. Biomaterials 25 (16), 3223–3232.
Ahmed, I., Lewis, M., Olsen, I., Knowles, J.C., 2004b. Phosphate glasses for tissue engineering: Part 1. Processing and characterisation of a ternary-based P2O5–CaO–Na2O glass system. Biomaterials 25 (3), 491–499.
Ahmed, I., Lewis, M., Olsen, I., Knowles, J.C., 2004c. Phosphate glasses for tissue engineering: Part 2. Processing and characterisation of a ternary-based P2O5–CaO–Na2O glass fibre system. Biomaterials 25 (3), 501–507.
Ahmed, I., Cronin, P.S., Abou Neel, E.A., Parsons, A.J., Knowles, J.C., Rudd, C.D., 2009. Retention of mechanical properties and cytocompatibility of a phosphate-based glass fiber/polylactic acid composite. J. Biomed. Mater. Res. B Appl. Biomater. 89 (1), 18–27.
Ahmed, I., Jones, I.A., Parsons, A.J., Bernard, J., Farmer, J., Scotchford, C.A., Walker, G.S., Rudd, C.D., 2011. Composites for bone repair: phosphate glass fibre reinforced PLA with varying fibre architecture. J. Mater. Sci. Mater. Med. 22, 1825–1834.
Ali Ashter, Syed, 2016. Processing biodegradable polymers. In: Introduction to Bioplastics Engineering. William Andrew Publishing, Oxford, pp. 179–209.
Athanasiou, Kyriacos A., Agrawal, Mauli, Barber, Alan, Burkhart, Stephen S., 1998. Orthopaedic applications for PLA-PGA biodegradable polymers. Arthrosc. J. Arthrosc. Relat. Surg. 14, 726–737.
Barbero, E.J., Lonetti, P., Sikkil, K.K., 2005. Finite element continuum damage modeling of plain weave reinforced composites. Compos. B Eng. 37 (2–3), 137–147.
Bauer, T.W., Schils, J., 1999. The pathology of total joint arthroplasty.II. Mechanisms of implant failure. Skelet. Radiol. 28, 483–497.
Carrasco, F., Gamez-Perez, J., Santana, O.O., Maspoch, M. Ll, 2011. Processing of poly (lactic acid)/organomontmorillonite nanocomposites: microstructure, thermal stability and kinetics of the thermal decomposition. Chem. Eng. J. 178, 451–460.
Chudoba, R., Vorechovsky, M., Eckers, V., Gries, T., 2007. Effect of twist, fineness, loading rate and length on tensile behavior of multifilament yarns (A multivariate study). Text. Res. J. 77 (11), 880–891.
Cox, Brain N., Flanagan, Gerry, 1997a. Handbook of Analytical Methods for Textile Composites. National Aeronautics and Space Administration.
Cox, B.N., Flanagan, G., 1997b. Handbook of Analytical Methods for Textile Composites. (NASA Langley Technical Report Server).
Faulstich De Paiva, Jane Maria, Mayer, Sergio, Cerqueira Rezende, Mirabel, 2005. Evaluation of mechanical properties of four different carbon/epoxy composites used in aeronautical field. Mater. Res. 8 (1), 91–97.
Felfel, R.M., Ahmed, I., Parsons, A.J., Haque, P., Walker, G.S., Rudd, C.D., 2012. Investigation of crystallinity, molecular weight change, and mechanical properties of PLA/PBG bioresorbable composites as bone fracture fixation plates. J. Biomater. Appl. 26 (7), 765–789.
Ferguson, S.J., Wyss, U.P., Pichora, D.R., 1996. Finite element stress analysis of a hybrid fracture fixation plate. Med. Eng. Phys. 18, 241–250.
Fibre-reinforced Plastic Composites-Determination of Flexural Properties. International Standard ISO 14125.
Fu, Q., Saiz, E., Rahaman, M.N., Tomsia, A.P., 2011. Bioactive glass scaffolds for bone tissue engineering: state of the art and future perspectives. Mater. Sci. Eng. C 31 (7), 1245–1256.
Gel Permeation Chromatography (GPC) - Part 1: Tetrahydrofuran (THF) Aselution Solvent. German Institute for Standardisation, DIN 55672-1-2007.
Gowda, R.V.M., 2010. Advances in yarn spinning and texturising. In: Alagirusamy, R., Das, A. (Eds.), Technical Textile Yarns - Industrial and Medical Applications. Woodhead Publishing Limited, Boca Raton Boston New York Washington, DC, pp. 56–90.
Goyal, D., Whitcomb, J.D., 2008. Load flow in plain woven composites. J. Compos. Mater. 42 (25), 2761–2777.
Guagliano, M., Riva, E., 2001. Mechanical behaviour prediction in plain weave composites. J. Strain Anal. Eng. Des. 36 (2), 153–162.
Han, N., Ahmed, I., Parsons, A.J., Harper, L., Scotchford, C.A., Scammell, B.E., Rudd, C.D., 2013. Influence of screw holes and gamma sterilization on properties of phosphate glass fiber-reinforced composite bone plates. J. Biomater. Appl. 27 (8), 990–1002.
Helene Bress, Inkle, Weaving, 1975. Flower Valley Press. Charles Scribner's Sons, Rockville, Maryland, U.S.
Ingeo™ Biopolymer 3251D Technical Data Sheet. NatureWorks LLC: Minnetonka, USA.
Jean, Launay, Hivet, Gilles, Duong, Ahn V., Boisse, Philippe, 2008. Experimental analysis of the influence of tensions on in plane shear behaviour of woven composite reinforcements. Compos. Sci. Technol. 68 (2), 506–515.
Jebastin Rajwin, A., Giridev, V.R., Renukadevi, M., 2012. Effect of yarn twist on mechanical properties of glass fibre reinforced composite rods. Indian J. Fibre Text. Res. 37 (4), 343–346.
K Naik, N., S Shembekar, P., 1992. Elastic behavior of woven fabric composites: I–Lamina analysis. J. Compos. Mater. 26 (15), 2196–2225.
Kim, H.W., Lee, E.J., Jun, I.K., Kim, H.E., Knowles, J.C., 2005. Degradation and drug release of phosphate glass/polycaprolactone biological composites for hard-tissue regeneration. J. Biomed. Mater. Res. B Appl. Biomater. 75 (1), 34–41.
Knowles, J.C., Franks, K., Abrahams, I., 2001. *Investigation of the solubility and ion release in the glass system K_2O-Na_2O-CaO-P_2O_5.* Biomaterials (22), 3091–3096.
Kravaev, Plamen, Stolyarov, Oleg, Gunnar Seide, Gries, Thomas, 2013. A method for investigating blending quality of commingled yarns. Text. Res. J. 83 (2), 122–129.
Kumar, Anil, Rakesh, K., 2003. Cupta, *mechanical properties*. In: Fundamentals of Polymer Engineering. Marcel Dekker, Inc., New York, USA, pp. 487–525.
Lauke, B., Bunzel, U., Schneider, K., 1998. Effect of hybrid yarn structure on the delamination behaviour of thermoplastic composites. Compos. Appl. Sci. Manuf. 29A, 1397–1409.
Lim, L.T., Auras, R., Rubino, M., 2008. Processing technologies for poly(lactic acid). Prog. Polym. Sci. 33 (8), 820–852.
Loewenstein, K.L., 1975. The manufacture of continuous glass fibres. Platin. Met. Rev. 19 (3), 82–87.
Long, A.C., Boisse, P., 2005. Mechanical analysis of textiles. In: Long, A.C. (Ed.), Design and Manufacture of Textile Composites. Woodhead Publishing Limited, pp. 62–109.
Lowenstein, K.L., 1973. The conversion of glass into glass fibre. The Manufacturing Technology of Continuous Glass Fibres. Elsevier Science Ltd., Amsterdam, pp. 86–190.
M Zhao, F., Takeda, N., 2000. Effect of interfacial adhesion and statistical fiber strength on tensile strength of unidirectional glass fiber/epoxy composites. Part. II: comparison with prediction. Composites Part A Applied Science & Manufacturing 31 (11), 1215–1224.
Mahmood, Ali Hasan, 2011. Optimising the lamination properties of textile composites. In: Engineering and Physical Sciences. University of Manchester.
Miao, Menghe, Christa Soong, Mei-Chun, 1995. Air interlaced yarn structure and properties. Text. Res. J. 65 (8), 433–440.
Middleton, John C., Tipton, Arthur J., 2000. Synthetic biodegradable polymers as orthopedic devices. Biomaterials 21, 2335–2346.
Naik, Rajiv A., 1994. Analysis of woven and braided fabric reinforced composites. J. Compos. Mater. 29 (17), 2334–2363.
Naik, R.A., 1995. Failure analysis of woven and braided fabric reinforced composites. J. Compos. Mater. 29 (17), 2334–2363.
Naik, N.K., Kuchibhotla, R., 2002. Analytical study of strength and failure behaviour of plain weave fabric composites made of twisted yarns. Composites Part A Applied Science & Manufacturing 33 (5), 697–708.
Naik, N.K., Madhavan, V., 2000. Twisted impregnated yarns: elastic properties. J. Strain Anal. Eng. Des. 35 (2), 83–91.
Naik, N.K., Singh, M.N., 2001. Twisted impregnated yarns: transverse tensile strength. J. Strain Anal. Eng. Des. 36 (36), 347–357.
Naik, N.K., Chandra Sekher, Y., Meduri, Sailendra, 2000. Polymer matrix woven fabric composites subjected to low velocity impact: Part I-damage initiation studies. J. Reinf. Plast. Compos. 19 (12), 912–954.
Parsons, Andrew J., Ahmed, Ifty, Haque, Papia, Fitzpatrick, Ben, Muhammad, I., Niazi, K., Walker, Gavin S., Rudd, Chris D., 2009. Phosphate glass fibre composites for bone repair. J. Bionics Eng. 6 (4), 318–323.
Patel, Nitesh R., Gohil, Piyush P., 2012. A review on biomaterials: scope, applications & human anatomy significance. Int. J. Emerg. Technol. Adv. Eng. 2 (4), 91–101.
Ramakrishna, S., Mayer, J., Wintermantel, E., Leong, Kam W., 2001. Biomedical applications of polymer-composite materials: a review. Compos. Sci. Technol. 61, 1189–1224.
Reinforcement Yarns-Determination of Linear Density. International Standard ISO 1889.
Reinforcement Yarns-Determination of Twist. International Standard ISO 1890.
Reinforcements–Woven Fabrics–Determination of Number of Yarns Per Unit Length of Warp and Weft. International Standard ISO 4602.
Rocher, J.E., Allaoui, S., Hivet, G., Gillibert, J., Blond, E., 2014. Experimental characterization and modeling of GF/PP commingled yarns tensile behavior. J. Compos. Mater. 49 (21), 2609–2624.

Scholz, M.S., Blanchfield, J.P., Bloom, L.D., Coburn, B.H., Elkington, M., Fuller, J.D., Gilbert, M.E., Muflahi, S.A., Pernice, M.F., Rae, S.I., Trevarthen, J.A., White, S.C., Weaver, P.M., Bond, I.P., 2011. The use of composite materials in modern orthopaedic medicine and prosthetic devices: a review. Compos. Sci. Technol. 71 (16), 1791–1803.

Södergård, A., Näsman, J.H., 1994. Stabilization of poly(l-lactide) in the melt. Polym. Degrad. Stab. 46 (1), 25–30.

Standard Test Mechod for Ignition Loss of Cured Reinforced Resin. ASTM D2584-11.

Tanoglu, M., Robert, S., Heider, D., Mcknight, S.H., Brachos, V., Gillespie, J.W., 2001. Effects of thermoplastic preforming binder on the properties of S2-glass fabric reinforced eposxy composites. Int. J. Adhesion Adhes. 21 (3), 187–195.

Taubner, V., Shishoo, R., 2001. Influence of processing parameters on the degradation of poly(L-lactide) during extrusion. J. Appl. Polym. Sci. 79 (12), 2128–2135.

Textile Glass-Yarns-Determination of Breaking Force and Breaking Elongation. International Standard ISO 3341.

Thompson, I.D., Hench, L.L., 1998. Mechanical properties of bioactive glasses, glass-ceramics and composites. Proc. Inst. Mech. Eng. H J. Eng. Med. 212 (2), 127–136.

Van Rijswijk, K., Van Geenen, A.A., Bersee, H.E.N., 2009. Textile fiber-reinforced anionic polyamide-6 composites. Part II: investigation on interfacial bond formation by short beam shear test. Compos. Appl. Sci. Manuf. 40 (8), 1033–1043.

Wisnom, M.R., Potter, K.D., 2007. 7 - understanding composite distortion during processing. In: C Long, A. (Ed.), Composites Forming Technologies. Woodhead Publishing, pp. 177–196.

Yu, Hengxing, Huang, Nanxun, Wang, Chaosheng, Tang, Zhilian, 2010. Modeling of poly (L-lactide) thermal degradation: theoretical prediction of molecular weight and polydispersity index. J. Appl. Polym. Sci. 88 (11), 2557–2562.

Zhang, Lu, Miao, Menghe, 2010. Commingled natural fibre/polypropylene wrap spun yarns for structured thermoplastic composites. Compos. Sci. Technol. 70 (1), 130–135.

Zheng, Nong Feng, Allen, Howard G., Moy, Stuart S.J., 1999. Study of stress concentrations in woven composites. J. Reinf. Plast. Compos. 18 (3), 198–214.

Zhu, Chenkai, 2016. Scale-up Manufacture and Characterisation of Resorbable Phosphate Based Glass Fibre for Textile Production. University of Nottingham, Nottingham, UK, pp. 33–91.

Zhu, Chenkai, Ahmed, Ifty, Parsons, Andy, Zakir Hossain, Kazi, Rudd, Chris, Liu, Jingsong, Liu, Xiaoling, 2017. Structural, thermal, in vitro degradation and cytocompatibility properties of P2O5-B2O3-CaO-MgO-Na2O-Fe2O3 glasses. J. Non-Cryst. Solids 457, 77–85.

Zhu, Chenkai, Ahmed, Ifty, Parsons, Andrew, Wang, Yunqi, Tan, Chao, Liu, Jingsong, Rudd, Chris, Liu, Xiaoling, 2018. Novel bioresorbable phosphate glass fiber textile composites for medical applications. Polym. Compos. 39, E140–E151.